JEE Journal of Ecological Engineering

Journal of Ecological Engineering, 2025, 26(11), 64–79
https://doi.org/10.12911/22998993/207662
ISSN 2299–8993, License CC-BY 4.0

Received: 2025.05.12
Accepted: 2025.08.01
Published: 2025.08.15

Concrete waste wash water recycling in geopolymer production – alkaline activated mortar

Waleed Nabeel Abu-Elayyan[1], Ayoup M. Ghrair[1*], Hussein Al-kroom[2]

[1] Water Resources and Environmental Management, Al-Balqa Applied University, Salt 19385, Jordan
[2] Department of Civil Engineering, School of Engineering, The University of Jordan, Amman, 11942, Jordan
* Corresponding author's e-mail: ayoup.ghrair@bau.edu.jo

ABSTRACT

Jordan faces significant water scarcity, with the ready-mix concrete industry being a major consumer of water and a contributor to environmental pollution. This study explores the recycling of concrete waste wash water for geopolymer production, offering a sustainable alternative to traditional Portland cement. The research investigates the optimal mix design by varying the ratios of waste wash water, metakaolin, sand, and fireplace ash across three stages, evaluating compressive and flexural strength, and analyzing microstructure and chemical composition. The methodology involved preparing geopolymer mortar samples with different compositions, testing their mechanical properties at 7, 28, and 90 days, and conducting XRD, XRF, and microstructure analyses. The results revealed that a 50% replacement of freshwater with waste wash water yielded the best performance, with further enhancements achieved by incorporating 41.7% metakaolin, 1.7% lime, and 40% fireplace ash. Microstructural analysis confirmed the formation of dense calcium silicate hydrate (C-S-H) gel, contributing to improved strength and durability. The findings demonstrate that concrete waste wash water and fireplace ash can be effectively utilized in geopolymer production, reducing environmental impact while maintaining high mechanical performance. This study provides a foundation for sustainable construction practices, addressing water scarcity and waste management challenges in Jordan and beyond.

Keywords: waste wash water, alkali, geopolymer, mortar, wood ash, Jordan.

INTRODUCTION

Jordan is among the most water-scarce countries globally, with per capita water availability of approximately 150 m³ per year – far below the 500 m³ threshold for absolute scarcity (Abualhaija et al., 2020; Ghrair et al., 2020). This scarcity is aggravated by rapid population growth, limited precipitation, inadequate water management, and shared groundwater resources (Al-Houri and Al-Omari, 2021; Kim et al., 2021). Non-conventional water sources, particularly treated wastewater, offer potential relief, yet their reuse is largely unregulated despite covering nearly 80% of the 80 MCM generated annually (Abualhaija and Mohammad, 2021; Almanaseer et al., 2020).

A major industrial consumer of freshwater in Jordan is the ready-mix concrete sector, which also generates large volumes of wastewater – estimated at 1.5 million m³ per year – containing alkalis and heavy metals from equipment washing (Ghrair et al., 2020; Radaideh, 2022). With no formal treatment protocols, this waste is often discharged untreated into natural systems, posing serious environmental hazards (Abualhaija et al., 2020). Internationally, similar practices incur heavy penalties, highlighting the need for sustainable management strategies (Peterson, 2019).

In parallel with water concerns, the cement industry contributes approximately 8% of global CO_2 emissions, prompting a shift toward low-carbon alternatives like geopolymer concrete (Chen et al., 2022; Ali et al., 2011). Geopolymers, first conceptualized in the 1970s, are alkali-activated materials synthesized from silica- and alumina-rich precursors (e.g., fly ash, slag, metakaolin) and alkaline activators such as NaOH or sodium silicate (Hassan et al., 2019; Cong and Cheng, 2021).

These binders offer superior mechanical strength, chemical resistance, thermal performance, and up to 80% lower CO_2 emissions compared to Portland cement (Ahmad et al., 2021; Elyamany et al., 2018; Luukkonen et al., 2018).

The key components of geopolymer concrete include low-calcium precursors (e.g., Class F fly ash, metakaolin), alkaline activators, and chemical admixtures to balance viscosity and strength. Admixtures such as naphthalene and polycarboxylate superplasticizers enhance workability (Abd Elmoaty et al., 2019). Additionally, incorporating solid wastes like fireplace ash – rich in CaO, SiO_2, and Al_2O_3 – has shown to improve strength and reduce landfill burden (Martínez-García et al., 2022; Li et al., 2019).

Recent research has highlighted the feasibility of using industrial waste streams – such as concrete wash water and wood ash – as viable components in geopolymer synthesis (Fan, 2020; Huo et al., 2021; Jwaida et al., 2023). High pH in wash water can benefit geopolymerization, while ash improves microstructure and compressive performance (Hamid and Rafiq, 2021). These developments align with the principles of circular economy, where waste materials are reintegrated into production cycles, contributing to environmental and economic sustainability (Naghizadeh et al., 2024; Krishna et al., 2021; Benhelal et al., 2013).

This study builds upon these findings by investigating the synergistic use of concrete waste wash water and fireplace ash in geopolymer mortar production. The goal is to optimize mix designs for enhanced mechanical and microstructural performance, offering a viable solution to both water scarcity and construction sustainability in Jordan and similar arid regions.

MATERIALS AND METHODS

Stage design

To achieve the goal of this thesis, which is to adjust the optimal ratios of the mixture to achieve the highest compressive strength, then held tests were conducted on 54 samples at the Arab Center for Engineering Studies (ACES). The samples were divided into three stages as illustrated in Figure 1, which explains the details of each stage. Each stage tested the compressive strength & flexural strength and then conducted microstructure analysis using SEM/EDX tests on the geopolymer

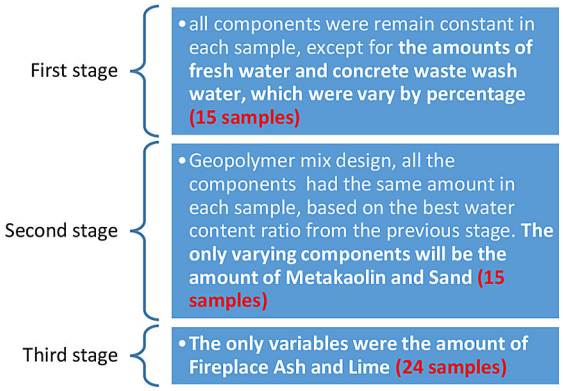

Figure 1. Number of stages and the variable elements in each stage

mortar samples, additionally, X-ray crystallography and X-ray fluorescence analyses. Finally, the mix design that performed the best is considered the new alkaline activated geopolymer concrete mix to replace Portland cement concrete.

Sampling and methods of analysis

Several samples of geopolymer mortar were prepared using specific materials and calculated masses as detailed in Table 1. The goal was to adjust the mixture's optimal ratios to achieve the highest compressive strength. In the initial geopolymer mix design stage, all components will remain constant in each sample, except for the amounts of fresh water and concrete waste wash water, which vary by percentage. This was intended to determine which sample exhibits the best mechanical properties. Then begin by using fresh water as 100% of the water component, then adjust the percentage to 75%, 50%, 25%, and 0%, while using 25%, 50%, 75%, and 100% of concrete waste wash water, respectively. 100% fresh water served as the control. Each geopolymer mortar sample, with a carefully measured mix design, that tested on the 7th, 28th, 90th, and 120th days, with three samples per mix design, totalling 15 samples.

To prepare Geopolymer/Alkaline Activated mortar using concrete waste wash water, metakaolin, local sand, and fireplace ash. The mortar was tested on the 7th, 28th, and 90th day for compressive and flexural strength. The test results were compared with Portland cement mortar samples of the same age. Additionally, microstructure analysis was conducted on the geopolymer mortar samples using SEM/EDX

Table 1. Stage number one in the samples mix design

No.	Metakaolin %	Gypsum %	Lime %	Sand %	Fireplace ASH%	Mixing water	
						Freshwater	Waste wash water
1	41.7	16.6	41.7	0	0	40	0
2	41.7	16.6	41.7	0	0	30	10
3	41.7	16.6	41.7	0	0	20	20
4	41.7	16.6	41.7	0	0	10	30
5	41.7	16.6	41.7	0	0	0	40

tests to study the chemical, mineralogical, and textural details. X-ray diffraction (XRD) analysis was also applied to identify the crystalline phases of the prepared geopolymers.

In the second stage of the Geopolymer mix design, all the components had the same amount in each sample, based on the best water content ratio from the previous stage. The only varying components were the amount of metakaolin and sand. This was done to determine which sample exhibits the best mechanical properties. The mixtures of metakaolin and sand that were used are as follows: (41.7, 0) for the control, (31.7, 10), (21.7, 20), (11.7, 30), and (0, 41.7). Each Geopolymer mortar sample with a measured mix design was tested on the 7th, 28th, 90th, and 120th day, with three samples per mix design, totaling 15 samples (Table 2).

In the third Geopolymer stage, all components had the same amount in each sample as shown in Table 3, based on the optimal water, metakaolin, and Sand percentages from previous stages. The only variables were the amount of fireplace ash and lime. This helped determine which sample exhibits the best mechanical properties. Then started by using fireplace ash as a 5% component, then increased the percentage to 10%, 15%, 20%, 25%, 30%, and 40%. These percentages correspond to 36.7%, 31.7%, 26.7%, 21.7%, 16.7%, 11.7%, and 1.7% of sand, respectively, with 41.7% Lime. A control sample with 0% sand and 41.7% lime was also compared. Each geopolymer mortar sample would undergo testing on the 7th, 28th, 90th, and 120th day, with three samples per mix design, totaling 25 samples.

Laboratory test

Materials used

Various materials were utilized in this study to detail the guidance for obtaining each material. Please refer to Tables 4 and Table 5 for the test locations.

Test specifications

Test specifications for the flexural and compressive strength of concrete have been conducted following the standards BS EN 196-1:2016, BS EN 12390-3:2019, and BS EN 12390-5:2019. The dimensions of the samples used are 15 × 15 × 15 cm for the cubes and 16 × 4 cm × [appropriate third dimension] for the beams.

X-ray crystallography and X-ray fluorescence analyses were conducted using the Panalytical Empyrean X-ray diffraction device and the Axios Minerals PW4400 X-ray fluorescence device,

Table 2. Stage number two in the sample mix design

No.	Metakaolin %	Gypsum %	Lime %	Sand %	Fire place ash %	Mixing water (50%)	
						Freshwater	Waste wash water
1	M	16.6	41.7	S	0	F	WW
2	M	16.6	36.7	S	5	F	WW
3	M	16.6	31.7	S	10	F	WW
4	M	16.6	26.7	S	15	F	WW
5	M	16.6	21.7	S	20	F	WW
6	M	16.6	16.7	S	25	F	WW
7	M	16.6	11.7	S	30	F	WW
8	M	16.6	1.7	S	40	F	WW

Table 3. Stage number three in the sample mix design

No.	Metakao-lin%	Gyps-um%	Lime%	Sand%	Firepla-ce ash%	Mixing water	
						Freshwater	Waste wash water
1	41.7	16.6	41.7	0	0	F	WW
2	31.7	16.6	41.7	10	0	F	WW
3	21.7	16.6	41.7	20	0	F	WW
4	11.7	16.6	41.7	30	0	F	WW
5	0	16.6	41.7	41.7	0	F	WW

Table 4. Materials obtained for the study

Material	Obtain guidance
Kaolin & metakaolin	Kaolin was collected from the Ma'an District (Butan Ghoul area) and then burnt in an oven at the University of Jordan at 95 degrees Celsius to produce Metakaolin.
Wood ash	By burning wood, a fireplace
Wash wastewater	From Al-Mamlka Concrete Company
Other material	By buying from the market

Table 5. The test location

Test	Location
Compressive & flexural strength	Arabic central for tests
Microstructure	University of Jordan at the cell therapy center
Electron microscope	Royal scientific society
X-ray crystallography (XRD) & X-ray fluorescence (XRF)	Royal scientific society

respectively. The analyses relied on the pressed pellets standard less method, which involves compressing a powdered sample into a dense, uniform pellet using a hydraulic press and a die set. This process ensures the sample is evenly distributed and compacted, which is crucial for obtaining accurate and reproducible analytical results.

Microstructural analysis, particularly using Scanning Electron Microscopy, is crucial for understanding the intrinsic properties and behavior of concrete. For more detailed images, Versa 3D utilizes focused ion beam scanning electron microscopy.

Compressive strength and flexural tests

On the 7th, 28th, 90th, and 120th days, the compressive and flexural strength of the samples (as shown in Figure 2 to 4) was evaluated by subjecting them to a load until failure at a rate of 1 kN/sec. tests done by concrete compression machine 1300 kN semi-automatic, Cyber Plus progress & flexural testing machine 150 kN from (MATEST). This test was conducted on both cube and beam samples, as shown in Figures 2 and 3, respectively. The compressive and flexural strength was calculated using the provided Equation 1. The test was repeated for various samples, and the average was calculated using Equation 1:

$$F = \frac{PL}{bd^2} \tag{1}$$

where: F – compressive strength (MPa), P – load at failure (KN), B – breath of the sample (mm), d – depth of the sample (mm)

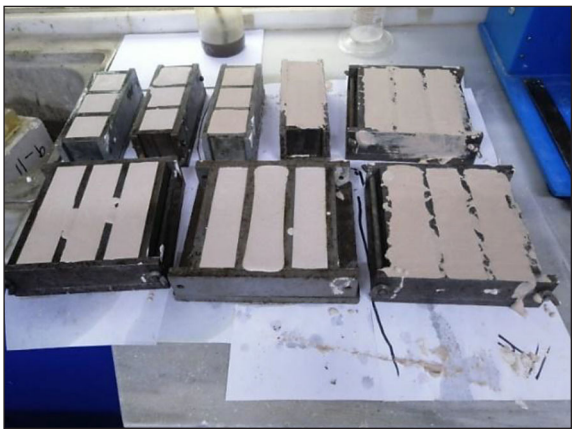

Figure 2. Prepare samples for tests

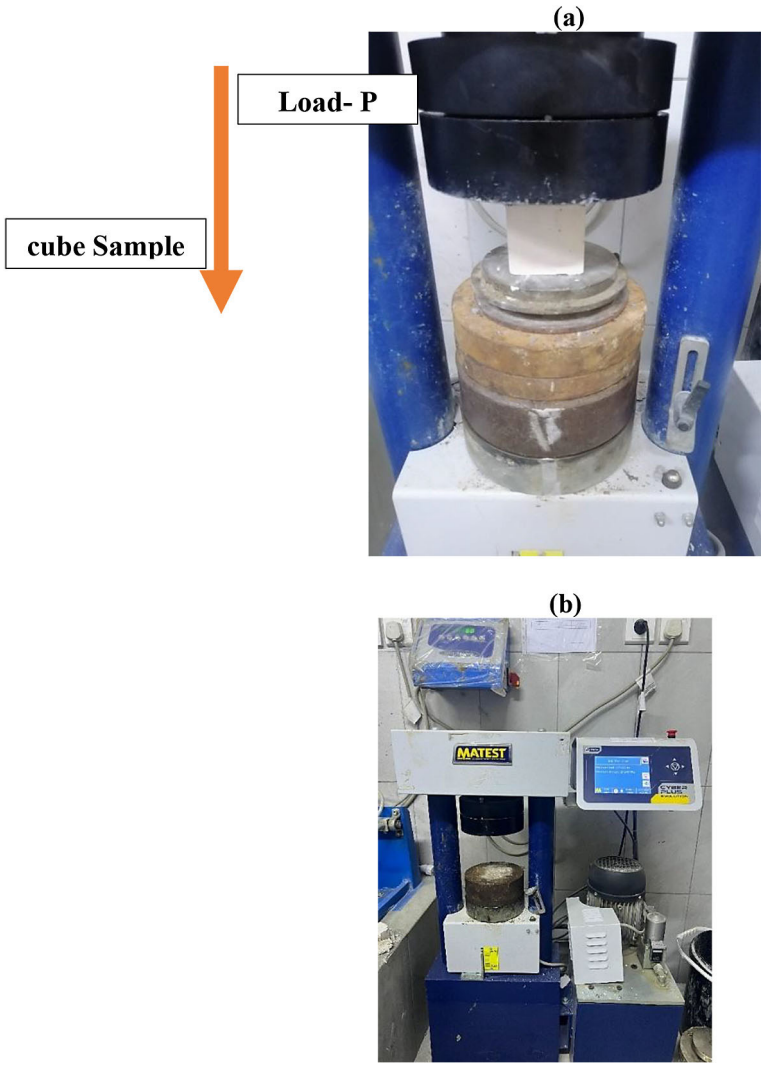

Figure 3. Compressive strength test for a cube (a), compressive strength machine for cube (b)

X-ray crystallography (XRD) and X-ray fluorescence (XRF)

XRD and XRF analyses were conducted to assess the mineralogical composition of the geopolymer mortars. These techniques are powerful tools for identifying the crystalline phases and chemical composition of various materials. The effectiveness of XRD and XRF analysis depends on several factors, including sample preparation, scanning range, scanning speed, and data analysis. Both methods work through the interaction of waves with crystalline materials, producing characteristic diffraction patterns that reveal the crystalline phases present in the samples. The difference between XRD and XRF is that XRD analyzes the crystal structure of materials, while XRF determines their elemental composition.

For the X-ray diffraction test, we obtained the results by grinding the powder sample after crushing the samples, which provided the best results across all stages. We then utilized a grain size of less than 40 microns and 70 microns for XRF and analyzed the sample using an instrument with a $\theta - 2\theta$ system, subsequently comparing the phases to acquire the final results.

X-ray crystallography and X-ray fluorescence analyses were conducted using the Panalytical Empyrean X-ray diffraction device and the Axios Minerals PW4400 X-ray fluorescence device, respectively.

Microstructure analysis

Microstructural analysis plays a vital role in evaluating the condition of concrete pavements. It enables the assessment of the internal structure and the identification of potential discontinuities through computed tomography scans. Furthermore, the density observed during microstructural

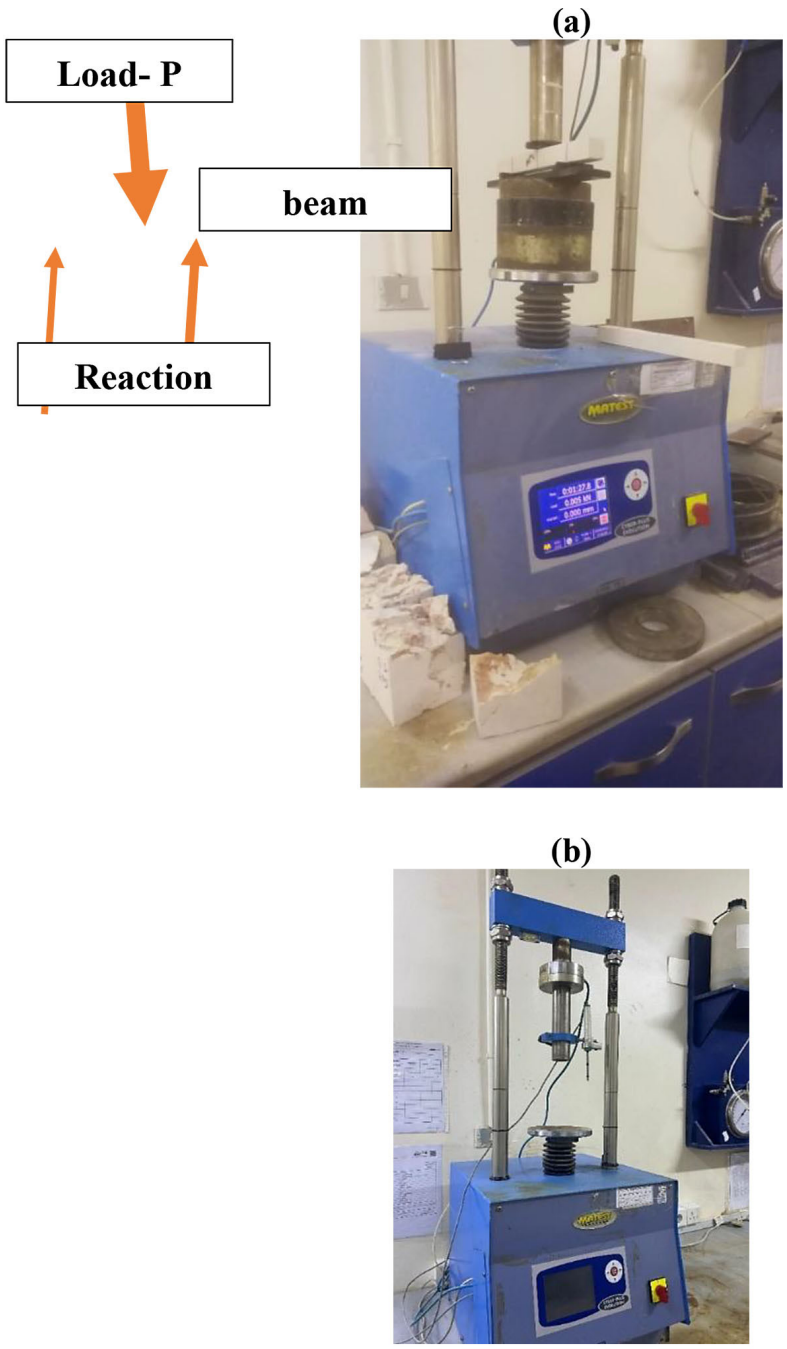

Figure 4. Flexural strength test for the beam (a), flexural strength machine for the beam (b)

analysis correlates with the compressive strength, indicating that denser structures exhibit higher strength. Proper sample preparation is of utmost importance, as sawn, unpolished and fractured surfaces often prove superior for revealing cracking patterns and crystal formations that may be obscured or destroyed by traditional polishing methods. To analyze the samples' microstructure, the samples that yielded the best results in all previous stages were analyzed using both an electron microscope and the Versa 3D instrument.

RESULTS AND DISCUSSION

Results of the first stage for compressive and flexural strength

The mortar samples underwent testing and analysis to measure their mechanical characteristics. Figures 5 and 6 below show display Laboratory results for strength for the compressive and flexural samples, where trials 1 to 5 show the different ratios of waste wash water (where: variables: the independent variable is the percentage

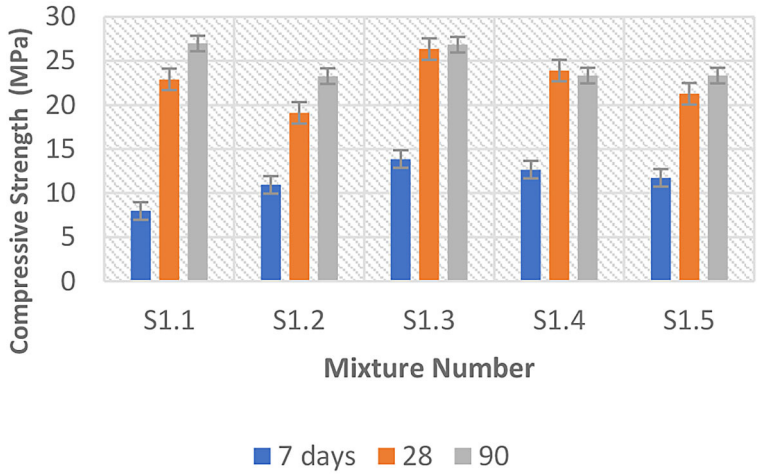

Figure 5. Comparison of compressive strength of first-stage mixtures over 7, 28 and 90 days

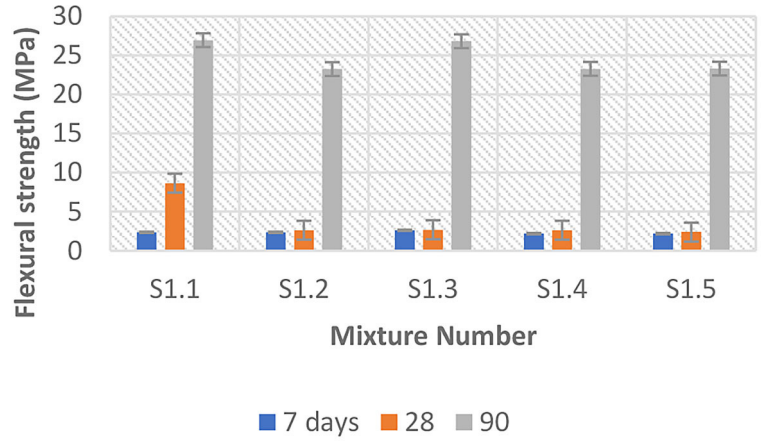

Figure 6. Comparison of flexural strength of first-stage mixtures over 7, 28 and 90 days

of fresh water replaced by concrete waste wash water. the dependent variables are the mechanical properties of the geopolymer mortar samples, measured through beam and cube tests at different curing periods; control: the control group uses 100% fresh water; samples: fifteen samples are prepared, each with a different mix design based on the percentage of fresh water and concrete waste wash water. Three samples are tested for each mix design).

At 7 days, the average flexural strength for the specimens ranged from 2.3 to 2.6 MPa, while the average compressive strength ranged from 7.9 to 13 MPa.

As the percentage of concrete waste wash water increases, the specimens' flexural and compressive strength slightly rise compared to the control sample (which used 100% freshwater). However, the differences in strength at this early stage of curing appear minimal. Compared to another researcher's findings at 7 days, the present study's specimens exhibited slightly lower flexural strength, while the compressive strength values were comparable (Purwanto et al., 2018).

After 28 days, the flexural strengths for the specimens range from 2.6 to 8.6 MPa, and for compressive for, the specimens range from 19 to 26 MPa. Similar to the 7-day results, there is a trend of slightly increasing compressive strength with higher percentages of concrete waste wash water. The difference in compressive strength between samples becomes more pronounced at this stage, suggesting potential long-term effects. Comparing the 28-day results to those reported by another researcher, the flexural strengths of the specimens in this study were found to be slightly lower, while the compressive strength values were similar (Purwanto et al., 2018). This difference may be attributed to the higher grade of concrete used in the other researcher's study.

For 90 days, the compressive strengths & flexural strengths for the specimens range from 23.3 to 26.9 MPa. After 90 days, the differences in compressive & flexural strength between samples are more noticeable. Samples containing higher percentages of concrete waste wash water continue to show similar or slightly higher compressive & flexural strengths compared to the control sample. Comparing the results from this study to those of other researchers who used similar materials, it was found that the flexural strength values were comparable, while the compressive strength values were consistent with the previous findings (Eloget et al., 2021; Mishra, 2019; Sathawane et al., 2013; Shoaei et al., 2019).

The compressive and flexural strengths of the geopolymer mortar samples are relatively low after 7 days, as the material is still undergoing initial hydration and setting. We observed variations in the samples, which could be due to differences in curing conditions, mixing consistency, or inherent material variability. At this early age, there is no clear trend regarding the influence of concrete waste wash water on strength.

The strength of mortar typically increases significantly by 28 days as a result of ongoing hydration and the formation of the cementitious matrix. It seems that certain mortar mix designs using waste wash water are comparable to the control group (using 100% fresh water). This implies that waste wash water from mortar can potentially be used to replace some fresh water without significantly affecting strength. Strength development continues, although at a slower rate compared to earlier stages. The variability in results persists, highlighting the importance of consistency in mixing and curing procedures.

When comparing the mixing ratio samples to the control sample, it was observed that using waste wash water resulted in a compressive strength nearly identical to that of the sample with 75% mixing water. Additionally, it demonstrated higher compressive and flexural strength than the control sample with 50% mixing water.

Results of the second stage for compressive and flexural strength

Figure 7 and 8 below show the results from the laboratory for both compressive and flexural samples, where trials 1 to 5 illustrate varying ratios of metakaolin and sand mixing amounts

The results indicate the following key points regarding compressive strengths and flexural strengths at different curing durations:

At 7 days, the flexural strengths for the specimens range from 5.8 to 19.6 MPa, while the compressive specimens show strengths between 6.7 and 18 MPa. On the other hand, at 28 days, the flexural strengths for the specimens range from 5.7 to 24 MPa, whereas the compressive strength for the specimens has strengths ranging from 7.8 to 20.73 MPa. Then, at 90 days, the flexural strengths of the specimens are between 9.3 and 25.03 MPa, and for compressive strength specimens, they range from 12 to 27.8 MPa.

To analyse these results, we need to consider the factors involved in the stage, which include the type of sample (compressive or flexural) and the duration of curing (7 days, 28 days, and 90 days).

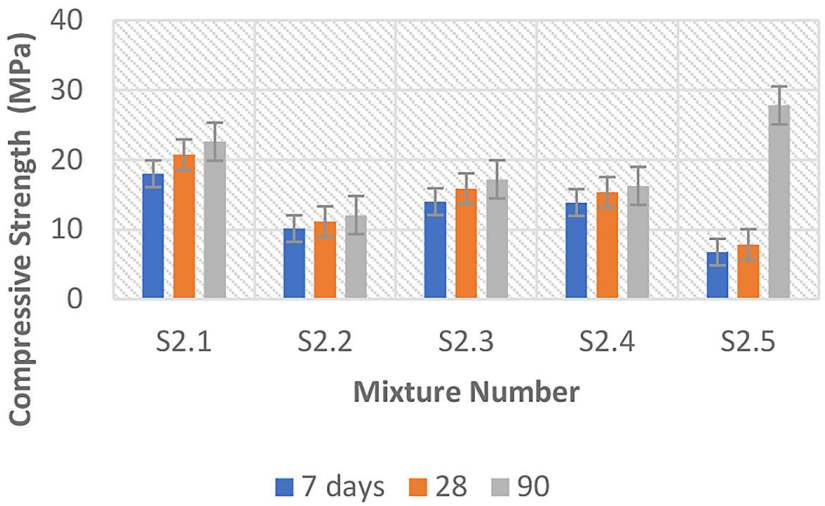

Figure 7. Comparison of compressive strength of 2nd-stage mixtures over 7, 28 and 90 days

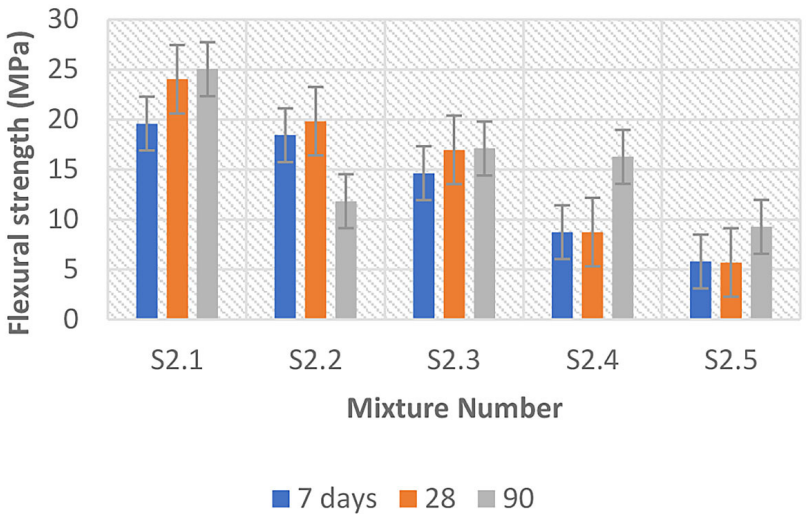

Figure 8. Comparison of flexural strength of 2nd-stage mixtures over 7, 28 and 90 days

At 7 days, both flexural and compressive strength for mortar specimens show relatively low strength, which is typical as mortar gains strength gradually over time. There is variation in strength across different mix designs, with those containing higher metakaolin content tending to exhibit slightly higher strengths, although the differences are not significant at this stage. Compared to previous studies, such as (Haruna et al., 2021), the compressive strength values reported in this work are relatively lower, potentially due to the utilization of concrete waste wash water as a mixing ingredient.

By 28 days, significant improvements in strength are observed across all mix designs as the mortar continues to gain strength during the curing process. Mix designs with higher metakaolin content generally demonstrate slightly better performance, particularly in compressive & flexural tests for the specimens compared to control samples that only have sand. The laboratory results indicate that the compressive and flexural strength values and development patterns of the mortar samples are similar to those reported in (Haruna et al., 2021) and other relevant studies. The control specimens containing only standard sand exhibited comparable performance to the samples incorporating a combination of metakaolin materials.

At 90 days, mortar strength further increases, although the rate of increase might start to slow down. Mix designs with higher metakaolin content continue to show better performance, though the differences might be diminishing over time. The variation in metakaolin and sand ratios influences the mechanical properties of geopolymer mortar. The strengths of geopolymer mortar increase significantly from 7 to 28 days, indicating the progress of pozzolanic reactions and the development of a more refined microstructure. Beyond 28 days, the rate of strength gain slows down, with strength reaching a plateau by 90 days. The laboratory results of this study are consistent with those reported by other researchers (Haruna et al., 2021; Kotwa and Spychał, 2019). They found that increasing the percentage and ratio of metakaolin can influence the early-age strength development of the mortar, particularly at 7 and 28 days. However, the optimal performance is observed at the 90-day testing period.

The relatively stable strengths observed at 90 suggest that the mixed designs have achieved a mature state. This stability is crucial for assessing the long-term durability and performance of geopolymer mortar structures.

It's noteworthy that compressive and flexural test specimens might exhibit slightly different strengths due to variations in stress distribution during testing. However, the overall trends in strength development should be consistent between the two types of specimens.

These results suggest that the choice of mix design can influence the mechanical properties of geopolymer mortar, with variations observed in both compressive and flexural strengths across different compositions and curing periods. Further experimentation and analysis may be needed to optimize mix designs for desired properties.

Results of the third stage for compressive and flexural strength

Figure 9 and 10 below display laboratory results for compressive strength & flexural samples, where trials 1 to 8 show different ratios of adding fireplace ash and lime. From the results above, we can highlight the following.

At 7 days, the compressive strengths of the beam specimens range from 5.6 to 19.88 MPa, while the cube specimens range from 5.33 to 19.33 MPa. While in at 28 days, the compressive strengths for the beam specimens range from 12.03 to 37.6 MPa, and for the cube specimens, they range from 9.6 to 34.26 MPa. On the other hand, at 90 days, the compressive strengths of the beam specimens range from 17 to 39.33 MPa, whereas the cube specimens range from 20 to 44.9 MPa. The compressive strength results obtained in this study are similar to those reported in previous research (Chithambaram et al., 2018; Hui-Teng et al., 2018)

Based on the data, samples with the highest lime ratio and the least amount of fire ash demonstrate the best compressive strength. Notably, mortar with a compressive strength exceeding 40 MPa is considered relatively high compared to normal mortar.

The optimal mixing ratio, substituting 50% of freshwater, demonstrated the most favourable outcomes in both flexural and compressive strength assessments during the initial stage. Further

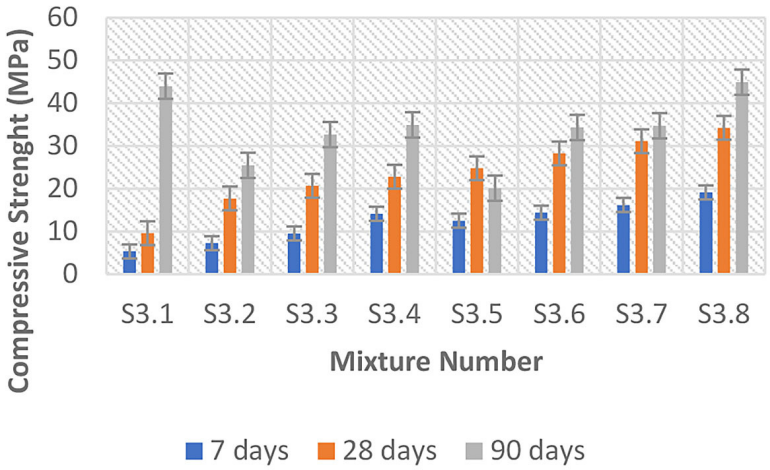

Figure 9. Comparison of compressive strength of third-stage mixtures over 7, 28 and 90 days

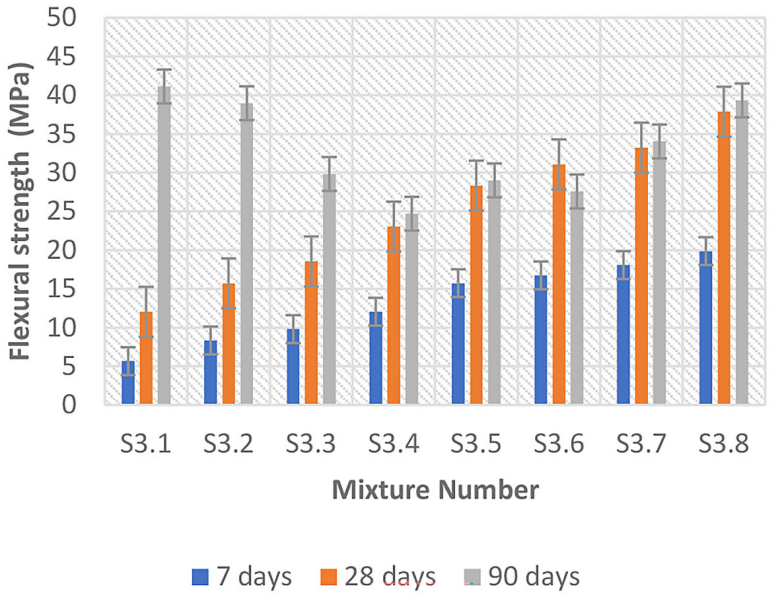

Figure 10. Comparison of flexural strength of third-stage mixtures over 7, 28 and 90 days

enhancements in stage two incorporated 41.7% metakaolin, followed by the addition of 1.7% lime and 40% fireplace ash in the third stage.

Results of the XRD, XRF and microstructure

Results for XRD analysis

Figure 11 and 12 below show the XRD analysis results for both the compressive & flexural test samples, which produced the highest compressive strength in the previous stages.

In the XRD results for flexural samples, calcite exhibits the highest percentage, 45%, followed by gypsum and quartz, 24.9% and 18.7%, respectively. There are also small percentages of dolomite, kaolinite, and brookite.

For the compressive samples, the XRD analysis results show that calcite has the highest percentage at 44.8%, followed by gypsum at 24.9% and quartz at 18.7%. There are also small percentages of dolomite, kaolinite, brookite, basanite, and ikaite.

XRD analysis for both flexural and beam samples was nearly identical, as both samples consist of the same mixed materials. The XRD results indicate the optimal mineral composition that contributes to the best compressive strength when using waste wash water.

Aligning with the findings reported in a previous study (Narloch et al., 2020) and other like (Wan et al., 2017), it can be seen that the additional components found may be forming polysialates due to the chemical composition of the water-wash used, the XRD analysis for both flexural and compressive test samples exhibit a nearly identical mineral composition, as the samples were comprised of the same mixed materials. The XRD results suggest that the optimal mineral makeup contributes to the highest compressive strength when incorporating waste wastewater.

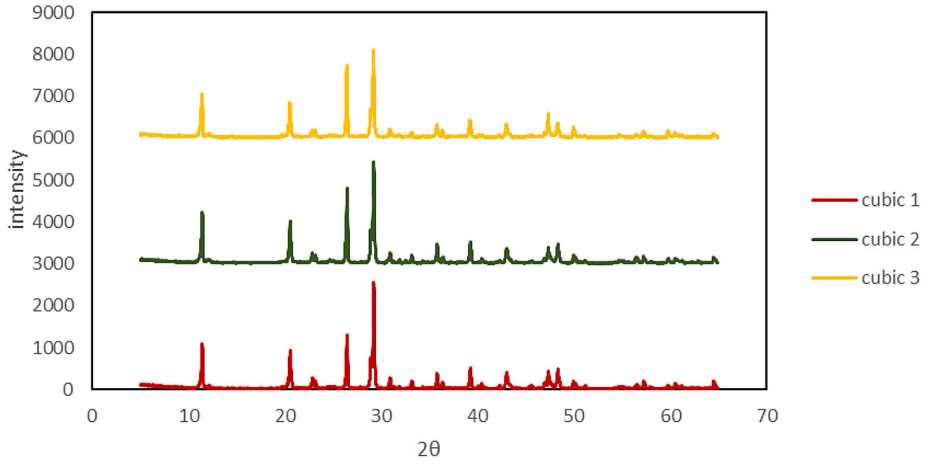

Figure 11. XRD analysis for compressive samples

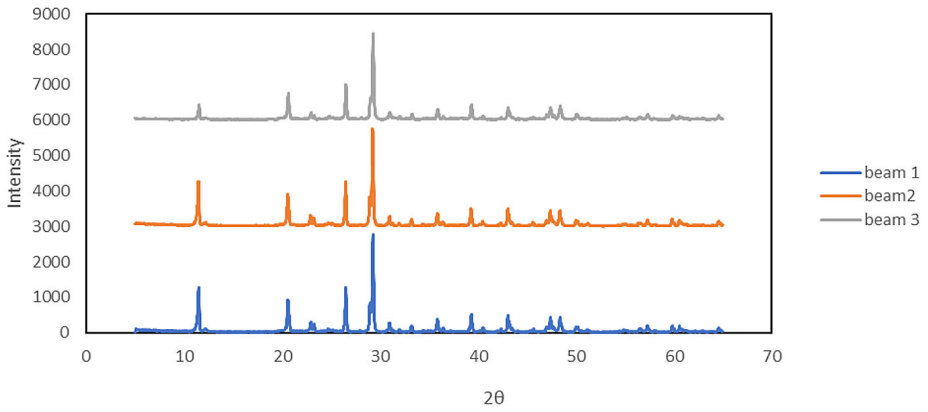

Figure 12. XRD analysis for flexural samples

There are common mineral components of mortar, water, and geopolymers, such as gypsum and calcite. However, there are also new components, like brookite and basanite, which can form even in small amounts.

Results for XRF analysis

The XRF analysis results for flexural indicate that CaO has the highest concentration at 45.6%, followed by SiO_2 at 23.8%. SO_3 accounts for 16.9%, while Al_2O_3 is at 10.26%. There are also small percentages of Fe_2O_3, MgO, Na_2O, K_2O, and P_2O_5 present.

The XRF analysis results for the samples indicate that the highest oxide present in the Compressive test samples is calcium oxide (CaO), which comprises 45.96% of the total. This is followed by silicon dioxide (SiO_2) at 23.6%. Sulfur trioxide (SO_3) accounts for 15.3%, while aluminium oxide (Al_2O_3) makes up 9.8%. Additionally, there are small percentages of iron (III) oxide (Fe_2O_3), magnesium oxide (MgO), sodium oxide (Na_2O), potassium oxide (K_2O), and phosphorus pentoxide (P_2O_5) in the samples. The XRF analysis indicates that the flexural samples exhibit a slight variation in oxide percentages compared to the beam samples. The flexural samples show higher concentrations of CaO, SiO_2, SO_3, and Al_2O_3, which contribute to the enhanced compressive strength. The XRF analysis results demonstrate that the sample's chemical composition is consistent with that of effective geopolymer materials, as evidenced by comparison with findings from prior studies (Jiang et al., 2018; Kürklü and Görhan, 2019; Silva et al., 2014)

The XRF test results for both the flexural and compressive samples are nearly identical, as both consist of the same mixed materials. These results indicate that the optimal oxide composition contributes to the highest compressive strength when utilizing waste wash water.

It has been observed that some unusual oxides, such as MgO, K_2O, and P_2O_5, are present in the samples. K_2O, or potassium oxide, can enhance the early strength development of mortar. P_2O_5, also known as phosphorus pentoxide, serves as a powerful dehydrating agent.

Results for microstructure analysis

The presented images depict the results of two microstructure analysis examinations conducted using an electron microscope (Figure 13) and the more detailed Versa 3D instrument (Figures 14 to 17).

The type, size, quantity, shape, and distribution of phases within a solid define its microstructure at the microlevel. The microstructure of concrete can be described through three key aspects: (i) hydrated cement paste, which consists of the hydration products resulting from the reaction between cement and water, primarily the calcium silicate hydrate (C-S-H) gel; (ii) pore structure, which encompasses gel pores, capillary pores, and voids; and (iii) the interfacial transition zone (ITZ), which delineates the boundaries between the cement paste and the aggregate particles.

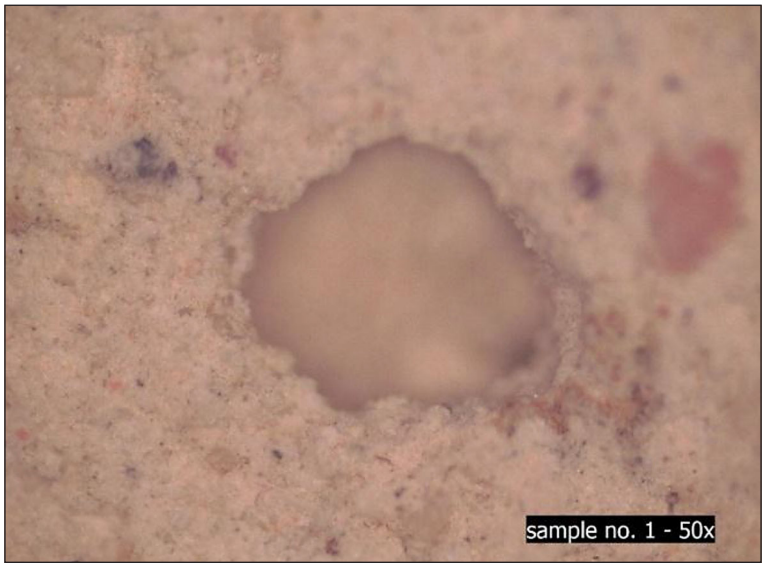

Figure 13. Electron microscope image of pores at close

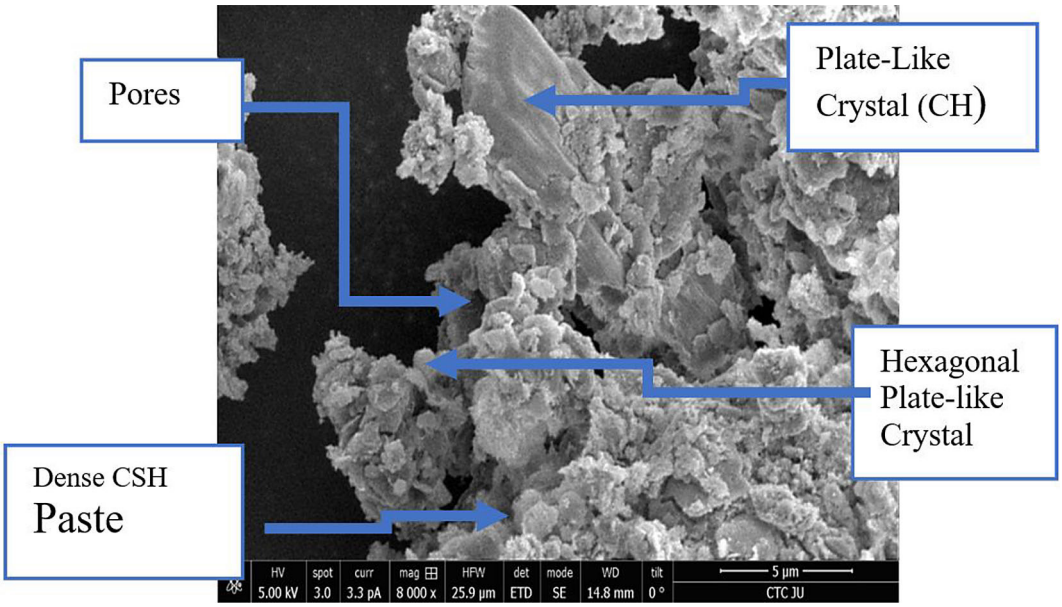

Figure 14. Microstructure image at 5 µm with pores measures

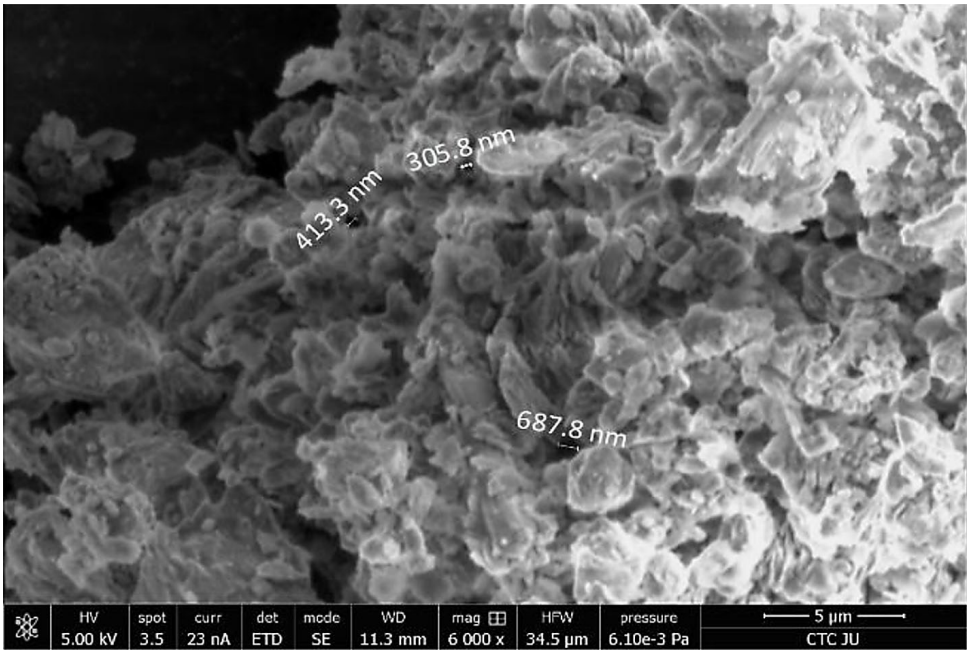

Figure 15. Microstructure image at 5 µm with pores measures

When analyzing microstructure, the characteristics of cement phases, supplementary cementitious materials, and other components play a crucial role.

The participants participated in the analysis of microstructures, component parts, component materials, and the effect of components on the analysis of microstructures.

It has been suggested that C-S-H displays a variety of microscopic shapes: (a) plate-like crystals; (b) irregular hexagonal panel crystals; and (c) dense C-S-H paste (refer to Figure 14). Regarding the volume of capillary voids in hydrated cement paste, this volume decreases as the w/c ratio decreases or as the hydration age increases.

The inclusion of fireplace ash results in a decreased pore proportion within the enlarged interfacial transition zone (ITZ), along with a reduction in calcium hydroxide (CH) crystals and ettringite formations. This addition has contributed to the observed presence of a denser calcium silicate hydrate (C-S-H) gel. Figure 14 illustrates

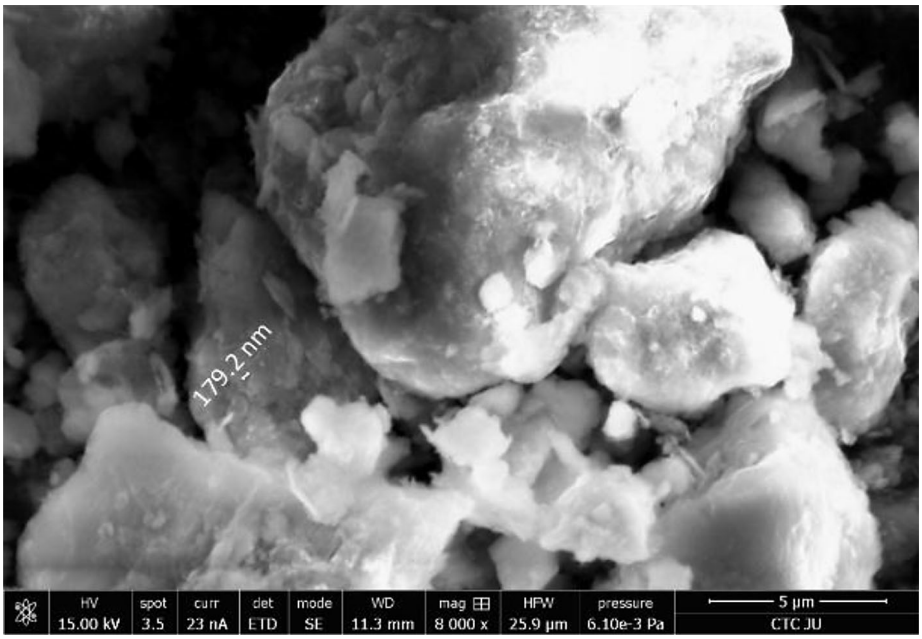

Figure 16. Microstructure image at 10 µm

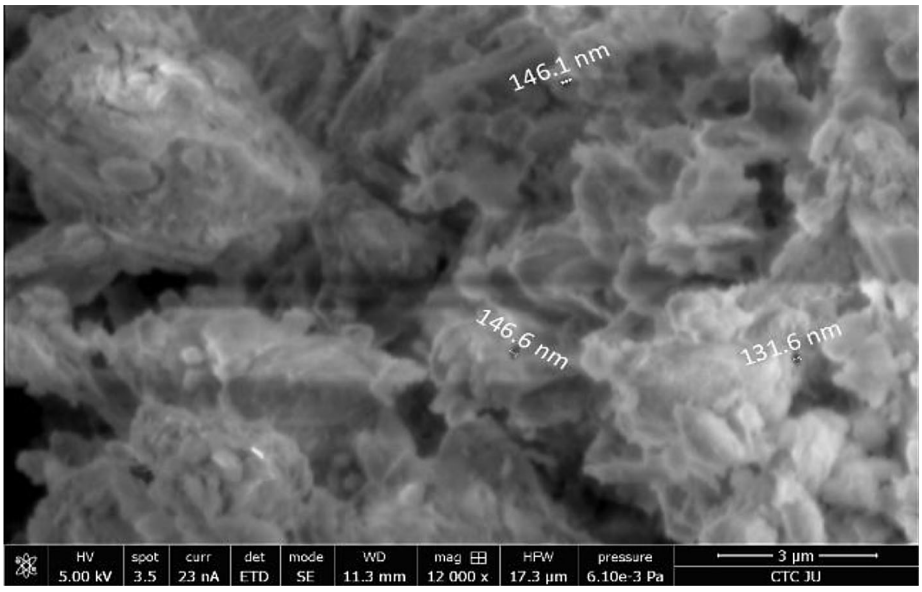

Figure 17. Microstructure image at 5 µm with pores measures

the hydrated cementitious products found in cement mortars treated with fireplace ash. Analysis of Figures 14 through 17 reveals the presence of both small and large crystals.

From this information, it can be concluded that the microstructure of high-performance mortar is microscopically more homogeneous and exhibits fewer defects compared to ordinary mortar.

Microstructural examination plays a crucial role in assessing the condition of concrete pavements. It facilitates the evaluation of the internal structure and the identification of potential discontinuities through a computed microscope scan. As illustrated in Figures 14 and 17, the scans reveal no apparent features or defects. Furthermore, the density observed during microstructural analysis correlates positively with the compressive strength, suggesting that denser microstructures exhibit enhanced structural integrity.

Comparing the results of microstructure investigations with other studies indicated a similar outcome, where the use of concrete waste wash water and fireplace ash achieved denser particle packing (Heinz, 2021; Kannan et al., 2017).

CONCLUSIONS

This study investigated the recycling of concrete waste wash water in the geopolymer/alkaline activated concrete production and the use of fireplace ash as a supplementary material. Results showed that concrete waste wash water can be efficiently treated and used in geopolymer/alkaline activated concrete. Not only can this approach solve the environmental issues caused by concrete waste wash water disposal, but also contribute to the sustainable management of water resources in Jordan.

The developed mortar showed good physical and chemical properties, making it suitable for various applications. Such properties include better compressive strength, lower permeability, and more resistance to aggressive substances, thus showing the opportunity of the geopolymer/alkaline activated concrete as a sustainable substitute to traditional Portland cement-based concrete. Addition of fireplace ash as a potential raw material in geopolymer/alkaline activated concrete has shown encouraging outcomes. In addition, this process is capable of recycling not only the solid waste from the landfill but also the concrete itself, which improves its properties, performance, and durability.

REFERENCES

1. Abualhaija, M M., Mohammad, A. (2021, October 1). Assessing water quality of Kufranja Dam (Jordan) for drinking and irrigation: Application of the water quality index. *Polish Society of Ecological Engineering, 22*(9), 159–175. https://doi.org/10.12911/22998993/141531
2. Abualhaija, M M., Hilal, A H A., Shammout, M W., Mohammad, A. (2020, March 30). Assessment of reservoir water quality using water quality indices: A case study from Jordan., 13(3), 397–397. https://doi.org/10.37624/ijert/13.3.2020.397-406
3. Ahmad L. Almutairi, Bassam A. Tayeh, Adeyemi Adesina, Haytham F. Isleem, Abdullah M. Zeyad. (2021, December). Potential applications of geopolymer concrete in construction: A review. *Case Studies in Construction Materials, 15*. https://doi.org/10.1016/j.cscm.2021.e00733
4. Al-Houri, Z., Al-Omari, A. (2021, November 24). Assessment of rooftop rainwater harvesting in Ajloun, Jordan. *IWA Publishing, 12*(1), 22–32. https://doi.org/10.2166/wrd.2021.064
5. Almanaseer, N., Hindiyeh, M., Al-Assaf, R. (2020). Hydrological and environmental impact of wastewater treatment and reuse on Zarqa River Basin in Jordan. *Environments, 7*(2), 14. https://doi.org/10.3390/environments7020014
6. Benhelal, E., Zahedi, G., Shamsaei, E., Bahadori, A. (2013). Global strategies and potentials to curb CO_2 emissions in the cement industry. *Journal of Cleaner Production, 51*, 142–161.
7. Chen, C., Xu, R., Tong, D., Qin, X., Cheng, J., Liu, J.,..., Zhang, Q. (2022). A striking growth of CO_2 emissions from the global cement industry is driven by new facilities in emerging countries. *Environmental Research Letters, 17*(4), 044007.
8. Chithambaram, S. J., Kumar, S., Prasad, M. M. (2018). *Study on the Effect of Sodium Hydroxide Concentration on Geopolymer Mortar.* In Lecture Notes in Civil Engineering 651. Springer Nature. https://doi.org/10.1007/978-981-13-3317-0_58
9. Cong, P., Cheng, Y. (2021). Advances in geopolymer materials: A comprehensive review. *Journal of Traffic and Transportation Engineering (English Edition), 8*(3), 283–314.
10. Eloget, M. O., Abuodha, S., Winja, M. M. O. (2021). The effect of sisal juice extract admixture on compressive and flexural strength of cement concrete. *Engineering Technology & Applied Science Research, 11*(2), 7041. https://doi.org/10.48084/etasr.4030
11. Elyamany, H. E., Abd Elmoaty, M., Elshaboury, A. M. (2018). Magnesium sulfate resistance of geopolymer mortar. *Construction and Building Materials, 184*, 111–127.
12. Fan, X. (2020, May 1). A Brief Introduction to the Research Status and Future Prospects on Geopolymer Concrete. *IOP Publishing, 508*(1), 012124–012124. https://doi.org/10.1088/1755-1315/508/1/012124
13. Ghrair, A., Heath, A., Paine, K., Al Kronz, M. (2020). Waste wash water recycling in ready mix concrete plants. *Environments, 7*(12), Article 108. https://doi.org/10.3390/environments7120108
14. Haruna, S., Mohammed, B. S., Wahab, M. M. A., Al-Fakih, A. (2021). Effect of aggregate-binder proportion and curing technique on the strength and water absorption of fly ash-based one-part geopolymer mortars. In *IOP Conference Series Materials Science and Engineering 1101*(1), 12022. IOP Publishing. https://doi.org/10.1088/1757-899x/1101/1/012022
15. Hassan, A., Arif, M., Shariq, M. (2019). Use of geopolymer concrete for a cleaner and sustainable environment – A review of mechanical properties and microstructure. *Journal of Cleaner Production, 223*, 704–728.
16. Hui-Teng, N., Cheng-Yong, H., Yun-Ming, L., Abdullah, M. M. A. B. (2018). The effect of various molarities of NaOH solution on fly ash geopolymer paste. In *AIP conference proceedings 2045*, 20098. American Institute of Physics. https://doi.org/10.1063/1.5080911

17. Huo, W., Zhu, Z., Chen, W., Zhang, J., Kang, Z., Pu, S., Wan, Y. (2021, July 1). Effect of synthesis parameters on the development of unconfined compressive strength of recycled waste concrete powder-based geopolymers. *Elsevier BV, 292*, 123264–123264. https://doi.org/10.1016/j.conbuildmat.2021.123264
18. Jwaida, Z., Dulaimi, A., Mashaan, N S., Mydin, M A O. (2023, May 23). Geopolymers: The green alternative to traditional materials for engineering applications. *Multidisciplinary Digital Publishing Institute, 8*(6), 98–98. https://doi.org/10.3390/infrastructures8060098
19. Kim, M., Hong, K.-S., Lee, J., Byeon, M., Jeong, Y., Kim, J. H., Um, W., Kim, H. G. (2021). Evaluating thermal stability of rare-earth containing wasteforms at extraordinary nuclear disposal conditions. *Nuclear Engineering and Technology, 53*(8), 2576. https://doi.org/10.1016/j.net.2021.02.025
20. Kotwa, A., Spychał, E. (2019). Parameters of mortars supplemented with chalcedonite powder. In *IOP Conference Series Earth and Environmental Science 214*, 12127. IOP Publishing. https://doi.org/10.1088/1755-1315/214/1/012127
21. Krishna, R. S., Mishra, J., Zribi, M., Adeniyi, F., Saha, S., Baklouti, S.,..., Gökçe, H. S. (2021). A review of developments of environmentally friendly geopolymer technology. Materialia, 20, 101212.
22. Luukkonen, T., Abdollahnejad, Z., Yliniemi, J., Kinnunen, P., Illikainen, M. (2018). One-part alkali-activated materials: A review. *Cement and Concrete Research, 103*, 21–34.
23. Martínez-García, R., Jagadesh, P., Zaid, O., Șerbănoiu, A. A., Fraile-Fernández, F. J., de Prado-Gil, J.,..., Grădinaru, C. M. (2022). The present state of the use of waste wood ash as an eco-efficient construction material: A review. *Materials, 15*(15), 5349.
24. Mishra, A. (2019). The study of flexural strength and durability of concrete using waste material. *International Journal for Research in Applied Science and Engineering Technology, 7*(6), 68. https://doi.org/10.22214/ijraset.2019.6016
25. Naghizadeh, L.N. Tchadjie & S.O. Ekolu, M.(2024). Circular production of recycled binder from fly ash-based geopolymer concrete. *Construction and Building Materials, 415* (0950–0618). https://doi.org/10.1016/j.conbuildmat.2024.135098
26. Peterson, P. (2019). Carwash regulations you need to know. https://www.carwash.com/carwash-regulations-need-know
27. Pilehvar, S., Cao, V. D., Szczotok, A. M., Carmona, M., Valentini, L., Lanzón, M.,..., Kjøniksen, A. L. (2018). Physical and mechanical properties of fly ash and slag geopolymer concrete containing different types of micro-encapsulated phase change materials. *Construction and Building Materials, 173*, 28–39.
28. Purwanto, P., Lie, H. A., Nuroji, Ekaputri, J. J. (2018). The influence of molarity variations on the mechanical behavior of geopolymer concrete. In *MATEC Web of Conferences 195*, 1010. EDP Sciences. https://doi.org/10.1051/matecconf/201819501010
29. Radaideh, J A. (2022, July 28). Status of Groundwater Resources in Jordan, 10(2), 59–67. https://doi.org/10.12691/ajwr-10-2-4
30. Shoaei, P., Musaeei, H. R., Mirlohi, F., Zamanabadi, S. N., Ameri, F., Bahrami, N. (2019). Waste ceramic powder-based geopolymer mortars: Effect of curing temperature and alkaline solution-to-binder ratio. In *Construction and Building Materials 227*, 116686. Elsevier BV. https://doi.org/10.1016/j.conbuildmat.2019.116686